International Journal of Adhesion & Adhesives 44 (2013) 200–208

Contents lists available at SciVerse ScienceDirect

International Journal of Adhesion & Adhesives

journal homepage: www.elsevier.com/locate/ijadhadh

Optical properties and UV-curing behaviors of optically clear PSA-TiO_2 nano-composites

Seung-Woo Lee [a], Ji-Won Park [a], Cho-Hee Park [a], Young-Eun Kwon [a], Hyun-Joong Kim [a,b,d,e,*], Eon-Ah Kim [c], Hang-Soo Woo [c], Steven Schwartz [d], Miriam Rafailovich [e], Jonathan Sokolov [e]

[a] Laboratory of Adhesion & Bio-Composites, Program in Environmental Materials Science, Republic of Korea
[b] Research Institute for Agriculture & Life Science, Seoul National University, Seoul 151-921, Republic of Korea
[c] Ulsan Fine Chemical Industry Center, Ulsan 681-802, Republic of Korea
[d] Department of Physics, Queens College, Flushing, NY 11367-1597, USA
[e] Chemical & Molecular Engineering, Department of Materials Science & Engineering, State University of New York, at Stony Brook, NY 11794-2275, USA

ARTICLE INFO

Article history:
Accepted 6 March 2013
Available online 15 March 2013

Keywords:
Optically clear PSA-TiO_2 nano-composites
Pressure sensitive adhesives
TiO_2
Optical properties
UV-curing behavior
Semi-IPN
Adhesion performance
Viscoelastic properties

ABSTRACT

Optically clear PSAs-TiO_2 nano-composites were investigated for the purpose of display. TiO_2 nano-particles can be directly incorporated into the polymer matrix to form high refractive index PSAs-nanocomposites films. Moreover, this study also employed semi-interpenetrated structured polymer network through the process of UV-curing with high refractive trifunctional acrylic monomer. The optical properties of PSAs-TiO_2 nano-composites were examined by using UV-visible spectroscopy and a prism coupler. Viscoelastic properties were obtained by ARES and adhesion performance was measured by the peel strength, probe tack and shear adhesion failure temperature. Furthermore, curing behaviors of the PSAs-TiO_2 nano-composites were investigated by using FTIR-ATR and gel content.

1. Introduction

A pressure-sensitive adhesive (PSA) is one that adheres instantly to a substrate by the application of light pressure. By pulling lightly, it also detaches easily and without residue [1,2]. In commercial products and industrial processes, acrylic PSAs are widely used because they are low-cost and exhibit properties like self-adhesiveness and high resistance to weathering and water. It is of interest to design acrylic PSAs in such a way that their adhesion can be adjusted according to their chemical structure [3–5] as well as external stimuli such as light [6] and heat [7–9]. Moreover, acrylic PSAs have several advantages which include excellent aging characteristics, resistance to elevated temperatures and plasticizer, exceptional optical clarity due to polymer compatibility and non-yellowing, highest balance of adhesion, cohesion and excellent water resistance [10]. Acrylic PSAs often include 3–10 wt% of acrylic acid and 90–97 wt% of alkyl soft acrylate is composed of butyl acrylate, hexyl acrylate, 2-ethylhexyl acrylate and isooctyl acrylate or decyl acrylate. Copolymers which contain butyl acrylate and acrylic acid are commonly used for the manufacture of acrylic PSAs with excellent adhesive performance [11].

Photo-induced reactions comprise of polymerization which is introduced by ultra-violet (UV) light, visible light, electron beam (EB) or laser. Photopolymerization science and technology has acquired considerable amount of attention due to its various industrial applications, such as inks, coatings, photoresists and pressure-sensitive adhesives (PSAs) [12–14]. Among the various methods of photo-curing, UV-curing systems are widely used due to their various advantages, such as rapid production rate in a small place of work, lower process costs, high chemical stability, high dimensional stability and solvent-free curing at ambient temperature [15].

Interpenetrating polymer networks (IPNs) are the subject of many current research interests due to the various technological applications that are possible. IPNs can be briefly defined as a combination of two incompatible polymer networks and at least one of it is synthesized and/or crosslinked in the presence of the other. Selection of different systems, such as polymerization by a combination of radical and cationic mechanisms is intended for the prevention of copolymerization and grafting reactions that may occur between the two polymer networks. This method was studied from an acrylate-based resin and an epoxy resin. The results showed that in the presence of a photosensitizer, the

* Corresponding author at: Laboratory of Adhesion & Bio-Composites, Program in Environmental Materials Science, 200-6204, Seoul National University, Seoul 151-921, Republic of Korea. Tel.: +82 2 880 4794; fax: +82 2 873 2318.
E-mail address: hjokim@snu.ac.kr (.-J. Kim).

0143-7496/$ - see front matter © 2013 Elsevier Ltd. All rights reserved.
http://dx.doi.org/10.1016/j.ijadhadh.2013.03.001

epoxide polymerization speeds up and within seconds two fully cured IPNs take place. It was reported on the curing behavior of novel IPNs formed an epoxy resin cured by anionic polymerization and a vinyl ester resin polymerized in the presence of various free radical initiators [16]. Moreover, the kinetics and properties of multifunctional acrylates which cross-link quickly by radical and cationic polymerizations have been investigated [17,18].

Titanium dioxide (TiO_2) fine particles with a unique color effect, UV-shielding characteristic, excellent chemical and thermal stabilities are commonly used in paints and inks which are based on polymer resin matrix. Moreover, TiO_2 particles can be used in optically clear pressure sensitive adhesives due to their high refractive index in spite of visible color. However, interfacial interactions between TiO_2 particles and most polymer matrices are poor. They possess great surface area and surface energy and as a result, TiO_2 particles are difficult to disperse into polymer matrix during paints and inks preparation. Moreover, they tend to clump and agglomerate [19].

Optical PSAs are being increasingly used in areas, such as LCDs, PDPs and OLEDs, due to the increase in the optical device production [20]. Optical PSAs should have high contrast, good clarity, high refractive index and good reliability [21]. The objective of this research is the fabrication of acrylic PSAs blending TiO_2 which can be applied to optical films. Firstly, acrylic PSAs based on a high refractive index material which is 2-phenxyethyl acrylate (2-PEA) were synthesized. Then, TiO_2 and tris[2-(acryloyloxy) ethyl] isocyanurate (TAEI) were blended together by using mechanical force. Emphasis was on the optical properties such as transmittance and refractive index. These properties were examined by using several instruments like UV-visible spectrometer and prism coupler. Secondly, UV-curing behaviors and adhesion performance were verified by peel strength, probe tack, shear adhesion failure temperature (SAFT), fourier transform infrared spectroscopy (FT-IR) and gel contents. Finally, surface morphology and viscoelastic properties were also observed by using contact angle, field emission scanning electron microscope (FE-SEM) and advanced rheometric expansion system (ARES).

2. Experimental

2.1. Materials

PSAs were synthesized by using 60 wt% 2-ethylhexyl acrylate (2-EHA, 99.0% purity, Samchun Pure Chemical Co., Ltd, Republic of Korea), 5 wt% acrylic acid (AA, 99.0% purity, Samchun Pure Chemical Co., Ltd, Republic of Korea) and 35 wt% 2-phenoxy ethyl acrylate (2-PEA, 90.0% purity, Tokyo Chemical Industry, Japan). Furthermore, ethyl acetate was used as the organic solvent at a boiling point temperature of about 78 °C. 0.1 wt%. 2,2′-azobisisobutyronitrile (AIBN, Junsei Chemical, Japan) was used as the thermal initiator to start radical polymerization. 2-hydroxy-2-methyl-1-phenyl-propane-1-one (Miwon Specialty Chemical, Republic of Korea) was used as the photoinitiator. Tris[2-(acryloyloxy)ethyl] isocyanurate (TAEI, Aldrich Chemical Co., Ltd, Republic of Korea) was used as the diluent monomer. Fig. 1 shows the chemical structure of trifunctional acrylate and it has six C=C double bonds.

2.2. Methods

2.2.1. Synthesis of binders

Acrylic PSAs were synthesized by solution polymerization and solid contents were around 40%. The mixture was placed into a 500 ml four-neck flask which was equipped with a stirrer, condenser and thermometer. The mixture was heated to a temperature of about 78 °C with constant stirring. Towards the end of the exothermic reaction, the temperature was maintained for about 1 h, and a blend of ethyl acetate and AIBN was also added. The reaction was allowed to proceed for 0.5 h and 2.5 h. Finally, polymerization was terminated by cooling the mixture to room temperature.

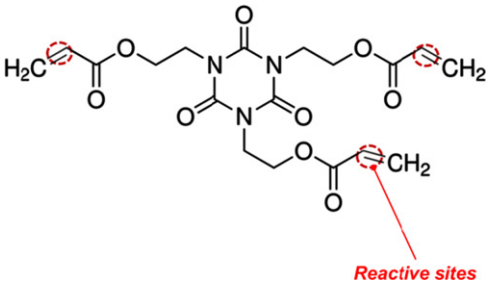

Fig. 1. Chemical structure of the Tris[2-(acryloyloxy)ethyl] isocyanurate (TAEI).

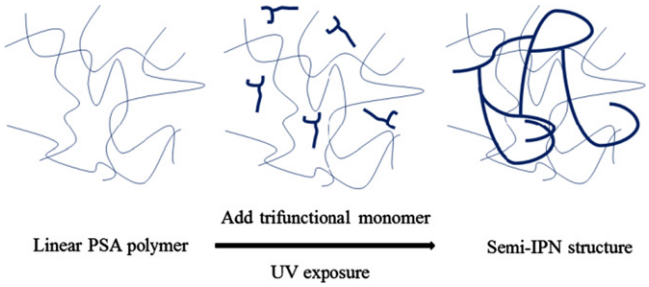

Fig. 2. Production process of semi-IPN structures in UV-cured acrylic PSAs [22].

2.2.2. Preparation of cured acrylic PSAs

UV-curable PSAs were prepared by blending the polymerized binders, a photoinitiator, TiO_2 and trifunctional monomer. The amount of TAEI monomer was 30 phr of the binder and the added photoinitiator was 2 phr of trifunctional monomer. At room temperature, the mixture was stirred for about 30 min by using a mechanical stirrer. The amount of TiO_2 was 0.1, 0.2, 0.5 and 1.0 wt%. The UV-curable polymers were coated onto the polyester films (PET, 50 μm thick, SKC, South Korea) by using a bar coater No. 18 (wet thickness 41.1 μm) and then, it was dried at 80 °C for 20 min. The UV-curable PSA films were cured by using a conveyor belt-type UV-curing equipment with a 100-W high-pressure mercury lamp (main wavelength: 340 nm). UV doses that were used in this study were 0, 200, 400, 800 and 1600 mJ/cm^2. UV doses were measured by using an IL 390C Light Bug UV radiometer (International Light, USA). Despite low molecular weights, the trifunctional monomers in the PSAs can be crosslinked after a UV dose and they form semi-IPN structures which are shown in Fig. 2.

2.2.3. Gel content

The gel content provides a degree of crosslinking. The weight of the samples was measured. Then, for 24 h the samples were immersed in toluene at room temperature, and the insoluble polymers were removed by filtration through a 200 mesh wire net. Then, the samples were dried at 70 °C until they reached a constant weight. The gel content was calculated by using the following equation:

$$\text{Gel content } (\%) = W_t/W_0 \times 100$$

where, W_0 is the weight before immersion, and W_{24} is the weight after immersion.

2.2.4. Dispersion characterization – particle sizes

Particle sizes and distribution of TiO_2 in samples were determined by using dynamic light scattering technique. (Nanotrac Ultra, Fashion Textile Center at Seoul National University).

2.2.5. Field-emission scanning electron microscopy observation

The surface morphology of each sample with different TiO_2 contents was measured by using the field-emission scanning electron microscopy (SUPRA 55VP, Fashion Textile Center at Seoul National University). The fractured samples were coated with a thin layer of gold (purity 99.99%) prior to the FE-SEM examination in order to prevent electron charging.

2.2.6. Optical properties

2.2.6.1. UV-visible spectroscopy. UV-visible spectroscopy (UV-1650PC Shimadzu, Japan) was used to examine the transmittance of the UV-cured acrylic PSAs. The bare PET for control and acrylic PSA sample which was coated on the PET film, were placed on the instrument. The transmittance was determined to be in the visible range of 380–700 nm.

2.2.6.2. Prism coupler. The refractive index of the acrylic PSAs which were coated on a PET film was detected by using a prism coupler 2010/M (Metricon, USA). Acrylic PSAs were UV-cured after coating the pre-polymers on the PET film in order to produce PSA films without cohesive failure. For reference a bare PET film was used. The prism and film were joined and the incidence angle of the laser beam was varied and so, the refractive index in both the thickness and plane directions can be determined.

2.2.7. Adhesion performance

2.2.7.1. Peel strength. The peel strength was also measured by using a Texture Analyzer. The specimens were prepared as 25 mn width samples. The specimens were pressed onto the stainless steel substrate by 2 passes of a 2 kg rubber and then, for over 12 h it was stored at room temperature. The peel strength was determined at 180° angle with a crosshead speed of 300 mm/min at 20° based on ASTM D3330. The peel strength is the average force on the debonding process. For five different runs, the force was recorded in g units and the average force was reported in g/25 mm.

2.2.7.2. Probe tack. The probe tack was measured at 20 °C by using a Texture Analyzer (Micro Stable Systems, TA-XT2i) with a 5 mm diameter stainless steel cylinder probe. The standard probe tack test was divided into the following three stages: approaching the surface of the PSAs, contact and detachment from the surface of the PSAs. The speed of the probe while approaching the surface of the PSAs was 0.5 mm/s, the contact time on the PSAs surface was 1 s under a 100 g/cm^2 constant force and the separation rate was 10 mm/s. In the debonding process, the probe tack was obtained at a maximum debonding force.

2.2.7.3. Shear adhesion failure temperature (SAFT). Shear adhesion failure temperature (SAFT) was measured by using a 1 in × 1 in. size sample that was attached to a stainless steel substrate by rolling with a 2 kg rubber roller twice. Then, the samples were stored at room temperature for 24 h. After loading with a 1 kg weight, the samples were held in the oven at a heating rate of 0.4 °C/min until it reached 200 °C. Moreover, the temperature when shear failure occurred was also recorded.

2.2.8. Contact angle test

The surface properties were measured by using a contact angle test. The surface energy was estimated from the water contact angle. Each sample was then, coated on stainless steel, polymethyl metacrylate, polycarbonate, glass substrate by using a 90 μm thickness applicator. The contact angle of acrylic PSAs which includes 0.5 phr of TiO_2 contents was measured by using a contact angle goniometer (SEO 300 A contact angle measuring device, Surface & Electro Optics Co., Republic of Korea).

2.2.9. Fourier transform infrared (FTIR) spectroscopy

IR spectra were recorded by using a Nicolet Magna 550 Series II FTIR spectrometer (Midac, USA) which is equipped with an attenuated total reflectance (ATR) accessory. In order to obtain the IR spectra of the UV-curable PSAs, each PSA was cut into 5×0.5 cm^2 pieces. In the ATR method, the thickness of PSAs is not important and so it was not measured. The ATR crystal was zinc selenide (ZnSe) and its refractive index at 1000 cm^{-1} was around 2.4. It had a transmission range of about 400–4000 cm^{-1}. The resolution of the spectra was 4 cm^{-1}.

The curing behavior of the UV-curable PSAs was analyzed by observing the changes in the deformation of the C=C bond at 810 cm^{-1}. Moreover, all the results were also obtained with a baseline correction and it was used to correct the spectra that had sloping or curved baselines.

3. Results and discussion

3.1. Dispersion characterization – particle sizes

As the process parameters in all the syntheses were equal, similar particle sizes and its distributions are expected. The most important key parameter that can have an effect on the distribution is the stirrer speed. Among other parameters for variation of particle distribution based on polymers are TiO_2 contents and viscosity [23].

In Fig. 3, a plot of the curve of particle size distribution is showed and this indicates the expectation. The mean of the particle size ranges from 2 to 4 nm distributions. The particle size in this range exerts effects on the adhesion performance. Hence, the difference in the optical properties and UV-curing behaviors can be obtained by not only polymer crosslinking but also by TiO_2 particles dispersion.

3.2. Field-emission scanning electron microscopy observation

Dispersion of fillers in a polymer matrix has significant effects on the properties such as adhesive properties, mechanical properties and so on. However, dispersion of inorganic fillers in polymer

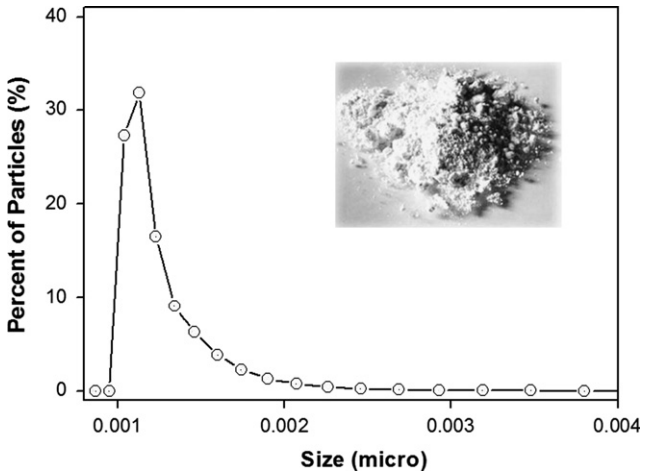

Fig. 3. Volume average particle size distribution of TiO_2 (0.5 phr in the acrylic binders).

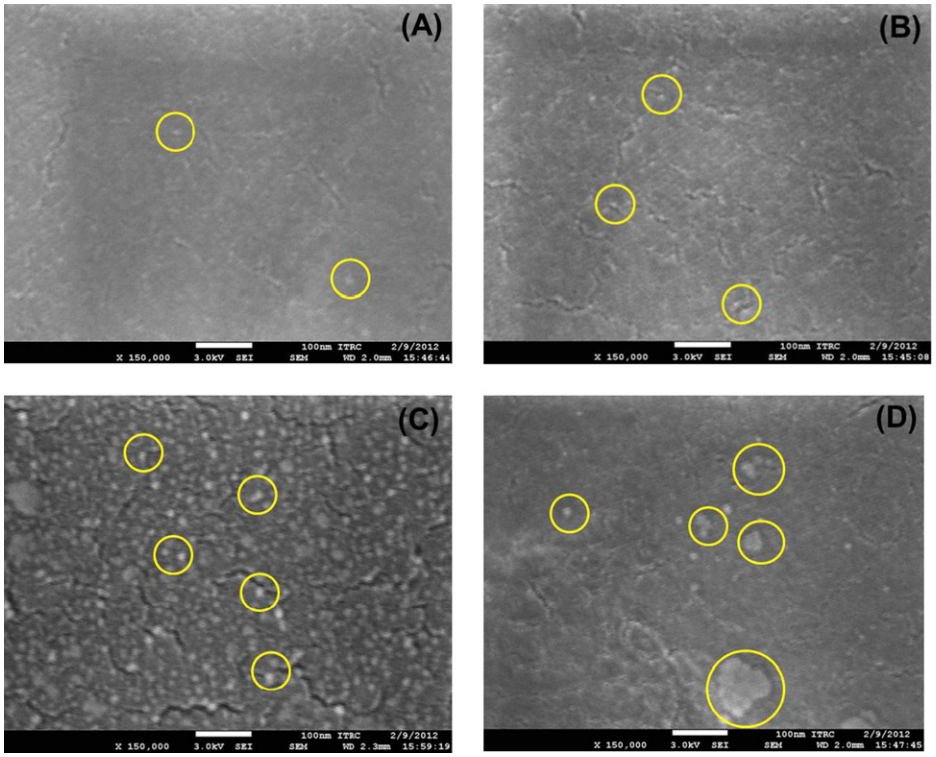

Fig. 4. Field-emission scanning electron images of acrylic PSAs with different TiO_2 contents (0.1 phr (A), 0.2 phr (B), 0.5 phr (C), 1.0 phr (D) in acrylic binders). The circles show raw TiO_2 particles. This implies that TiO_2 has a strong tendency to self-agglomerate (D). Therefore by increasing TiO_2 contents, optical properties, adhesion performance and UV-curing behaviors will vary. Furthermore, it has a strong effect on the optical properties due to its raw color, reflectiveness and difficult dispersion in acrylic PSA.

is not an easy process and this is due to the weak interfacial interaction between the polymer matrix and fillers. In other words, inorganic fillers have a strong tendency to self-agglomerate [23]. Fig. 4 shows FE-SEM images of acrylic PSAs with different TiO_2 contents. Most of the raw TiO_2 particles seriously agglomerate in image (D), while self-agglomerate tendency reduces in image (C). Due to the well-dispersed TiO_2 particles, the TiO_2 particle surface has been inserted organic components and this can increase the interaction between TiO_2 and polymer matrix.

3.3. Gel content

In order to determine the degree of curing of acrylic PSAs, the gel content was calculated by measuring the insoluble material that was left behind [24]. Amount of gel phase that was measured is defined as the amount of both crosslinked molecules as well as highly entangled and coiled polymer molecules. In the latter case, crosslinking occurs only through entanglement. Moreover, it is truly not a polymeric network which usually consists of interconnected polymeric molecules. Therefore, the gel phase can be varied due to the change in the polymer molecular weight [25,26], or due to the increased crosslinking density. In this study, only UV induced crosslinking should affect the amount of gel phase as the initiator concentration, the temperature and humidity profiles were equal for all the samples. Similar increase in the gel phase amount was also acquired from our previous study where, the crosslinking of polymer molecules was induced by an addition of the multifunctional acrylic monomer in the polymerization phase [26]. Not only the molecular weight but also the crosslinking density may be explained as a most important factor in the adhesion property. Moreover, the mobility of the polymer molecules is strongly reduced by the chemical bond in the polymer structure [27].

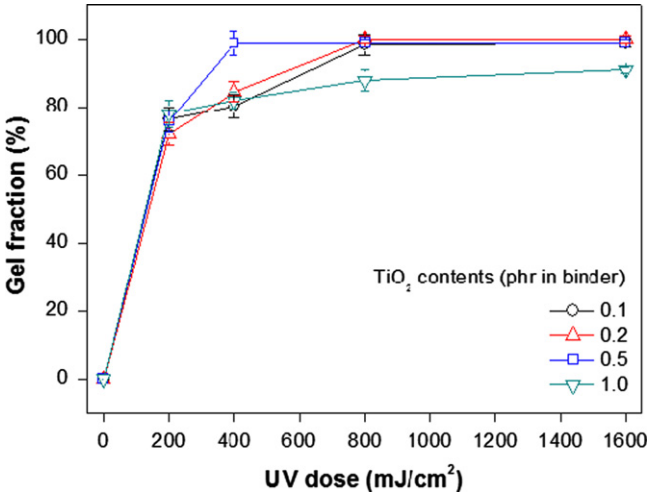

Fig. 5. Gel fraction of UV-curable acrylic PSAs with different TiO_2 contents.

In Fig. 5, it is clearly presented that the gel content of the acrylic PSAs with different TiO_2 contents increased with an increasing UV dose. However, the gel content of the acrylic PSAs with 0.5 phr of TiO_2 has indicated almost 100% from 400 dose and it is relatively constant compared to the other samples. This shows that the acrylic PSAs with 0.5 phr of TiO_2 has a higher probability of forming entanglements and crossliked structures due to its well-dispersion.

3.4. FTIR-ATR spectroscopy

The UV-curing kinetics of the photoinduced cross-linking was observed by using FTIR-ATR spectroscopy. After photoinitiation

by UV irradiation at a specific wavelength, the functional monomers proceeded to polymerize. Moreover, these functional monomers formed a crosslinked structure. The curing behavior of the functional monomers can be explained by using FTIR-ATR as the C=C twisting vibration in the functional monomers participates in the cross-linking reaction. These double bonds have a plane conformation but UV irradiation deforms them into an out-of-plane conformation [17].

In this study, the UV curing behavior of the acrylic PSAs that were blended with TAEI was observed by using FTIR-ATR spectroscopy. After the reaction between C=C bonds of TAEIs through radical polymerization, the acrylic PSA cured and then, it formed a semi-IPN structure. Therefore, the kinetic profile of UV crosslinkable PSAs can be explained by the evaluation of the absorption band at 810 cm^{-1}. In this study, the characteristic signal that was used for calculation was at 810 cm^{-1} and it was integrated to determine the decrease of the concentration of the C=C bonds as a function of the UV dose. The concentration of C=C bonds as function of the UV dose was calculated by using the following equation:

$$\text{Conversion of UV–cured group } (\%) = \frac{(A_{810})_0 - (A_{810})_t}{(A_{810})_0} \times 100$$

Where, $(A_{810})_0$ is the IR absorbance at 810 cm^{-1} before UV irradiation and the $(A_{810})_t$ is the IR absorbance at 810 cm^{-1} after UV irradiation. Fig. 5(A) shows the FTIR-ATR spectra at 810 cm^{-1} of PSAs. These spectra were collected at different UV doses (range from 0 to 1600 dose). It can be observed that the characteristic signal at 810 cm^{-1} gradually decreased with an UV dose. Integration of the characteristic signals gathered in Fig. 5(A), indicates results that are presented in Fig. 5(B). From Fig. 5(B), the change in the concentration profile can be seen, The UV dose for optimal crosslinking is approximately at least 800 mJ/cm^2. From this point on, only a minor change in the C=C concentration can be observed. UV light can potentially decompose the C=C bonds in the polymer or monomer. But, the conversion was not 100%. The remaining C=C bonds may have remained unreacted after the action of the photoinitiator as they were trapped in the crosslinked polymer network [13] Fig. 6.

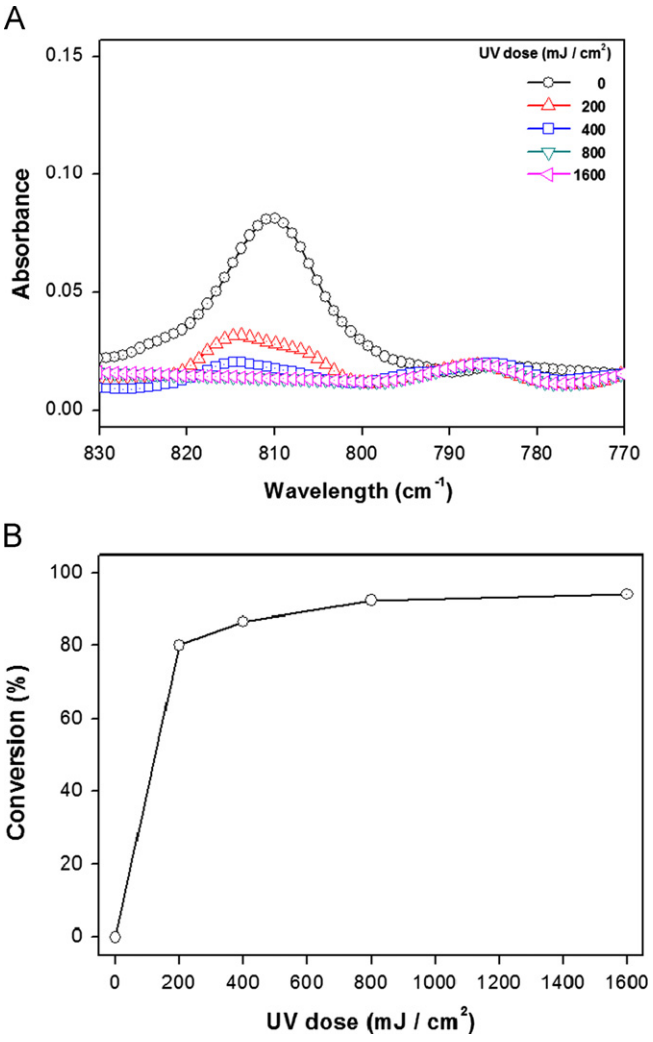

Fig. 6. FTIR-ATR spectra of UV-curable acrylic PSAs with different UV doses (A) and change of concentration of C=C bonds as a function of dose (from 0 to 1600 dose) for UV-curable acrylic PSAs with 0.5 phr TiO_2 in binders (B).

3.5. Optical properties

3.5.1. UV-visible spectrometer

Organic–inorganic hybrid materials have acquired considerable attention due to their novel physical and chemical properties. Incorporation of the nanoparticles into the polymer matrix becomes the most common method in production. The dispersion property of TiO_2 nanoparticles in the polymer matrix becomes a critical issue in the successful preparation of these transparent materials. Moreover, particle agglomeration can also significantly reduce the transparency [28]. The transmittance of acrylic PSAs with different TiO_2 contents was obtained by using the UV-visible spectroscopy. Acrylic PSAs should indicate high transmittance ($>95\%$) that is to be used in optical films. In this study, acrylic PSAs were coated on a PET film. The bare PET film was employed as the reference. In Fig. 7(A), minor difference were shown that the transmittance of samples which include from 0.1 to 0.5 phr of TiO_2 in binders. But, the transmittance of acrylic PSA with 1.0 phr of TiO_2 was $<90\%$ due to particle agglomerations. In our previous study, the successful optical PSA should indicate $>95\%$ of transmittance. For this reason, UV-curing was employed at a sample with 0.5 phr of TiO_2 to form a crosslinked structure. In Fig. 7(B), the transmittance was gradually increased by increasing the UV dose to 400 mJ/cm^2. But at 800 and 1600 dose, the transmittance was obviously decreased as excessive UV irradiation may have been influenced on not only crosslinking but also polymer deformation. Hence, the UV dose required for a successful transmittance is approximately 400 dose.

3.5.2. Prism coupler

Inorganic nanoparticles can be embedded in the polymer matrix to form highly refractive index materials [28]. The refractive index of a polymer that contains a high refractive index functional group is higher compared to that of the monomer. This indicates that the PEA in all binders, which had the high refractive index of 1.518, shows the higher refractive index of the polymer due to the presence of phenyl group [21]. Fig. 8 shows the refractive index distributions of the acrylic PSAs with 0.5 phr of TiO_2 in binders and also in the different UV doses. Minor differences which were observed in this result indicate that the UV crosslinked structures can increase the refractive index. All samples with UV doses exhibit excellent refractive property in the visible region.

3.6. Contact angle test

The surface energy of a range of materials which use contact angle measurements and Young's equation was analyzed [29]. The common liquid that is used for the calculation of surface energy is water, as it has a surface tension of 76 mN/m. The solid surface is

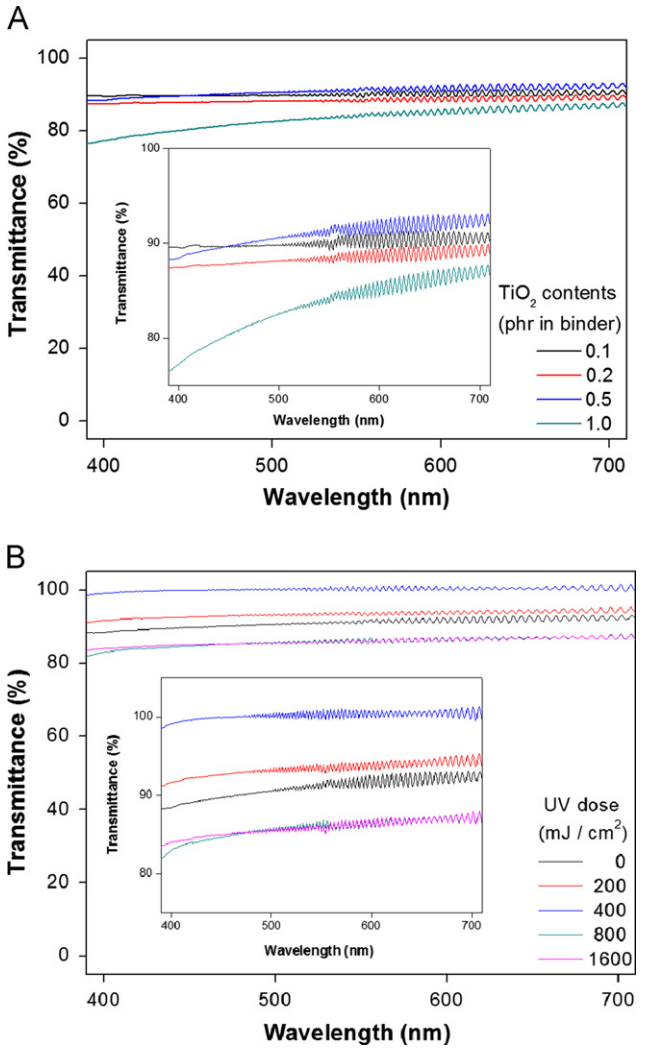

Fig. 7. Variations in the transmittance of acrylic PSAs' film, 380~700 nm (with TiO_2 content of 0.1, 0.2, 0.5 and 1.0 phr in binders (A), with UV dose of 0, 200, 400, 800 and 1600 mJ/ cm^2 at 0.5 phr of TiO_2 in binders (B)).

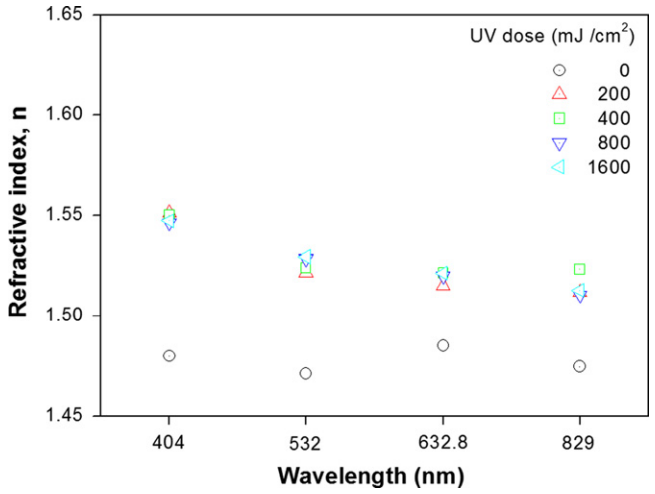

Fig. 8. Variation in the refractive index of the acrylic PSAs' film with 0.5 phr of TiO_2 (with UV dose of 0, 200, 400, 800 and 1600 mJ/cm^2) in the wavelength range of the visible region.

hydrophilic and this indirectly demonstrates that the surface has high surface energy if the contact angle of water on a solid surface is $<90^\circ$. Compared to a hydrophilic surface, a hydrophobic surface

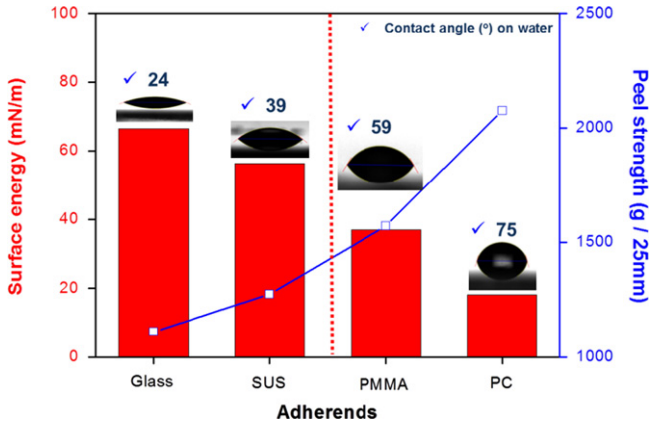

Fig. 9. Relation between the surface energy of water on different substrates which are glass, stainless steel (SUS304), polymethylmethacrylate (PMMA) and polycarbonate (PC) and peel strength of the acrylic PSAs containing 0.5 phr of TiO_2 in binders.

has a water contact angle $>90^\circ$ and it is believed to have a low surface energy [30]. Moreover, in Fig. 9, the relation between the surface energy of four substrates which are glass, stainless steel (SUS304), polymethylmethacrylate (PMMA) and polycarbonate (PC) and peel strength of the acrylic PSAs that contain 0.5 phr of TiO_2 in binders are shown. The peel strength of the acrylic PSAs was increased with the decrease in the surface energy of substrates and this may indicate that the acrylic PSAs was more hydrophobic compared to water. Fox and Zisman indicated that it was attributed to the surface energy of PSAs except for the roughness effect of the surface [30].

3.7. Adhesion performance

In this study, three basic adhesion properties, peel strength, tack and shear adhesion failure temperature, were controlled by the UV doses and TiO_2 contents. Moreover, the UV dose can be handled by adjusting the power of the lamps and/or the speed at which the substrate is passed under lamps in the production plant. The solvent borne UV-crosslinkable acrylic PSAs are directly coated. After removing the solvents the adhesive film is crosslinked by UV-irradiation and in a transfer process, depending on the carrier material, to produce the adhesive properties as required [6]. Generally, the adhesion performance of acrylic PSAs depends on not only their viscoelastic properties but also on the dispersion of TiO_2 particles in the polymer matrix. Furthermore, in order to optimize PSAs properties, the sufficient bond strength and clean removability are the two essential factors. It requires the maintenance of sufficient bonding strength to avoid detaching of the optical films. Moreover, it requires clean removability from the specific adherend when optical films are removed or replaced due to wrong-position or other failure issues. These factors can be influenced by the chemical composition, crosslinking density and inorganic fillers [31,32]. Peel strength of acrylic PSAs which are attached on glass, SUS, PC and PMMA with different TiO_2 contents are shown in Fig. 10. In Fig. 10(A) and (B), peel strength increased at the content of 0.1 phr of TiO_2 in binders and this is due to the increased cohesion of PSAs matrix. On the other hand, lower peel strength values may be attributed to the improved cohesive strength of the PSAs which has an effect on the degree of deformation. Hence, this causes lower force that is required for debonding process. When TiO_2 particles were not loaded into PSAs matrix, slightly cohesive failure occurred but this cohesive failure disappeared as the contents of TiO_2 increased [33]. Minor differences suggested that the peel strength of samples which include from 0.1 to 1.0 phr of TiO_2 in binders, indicate almost the same

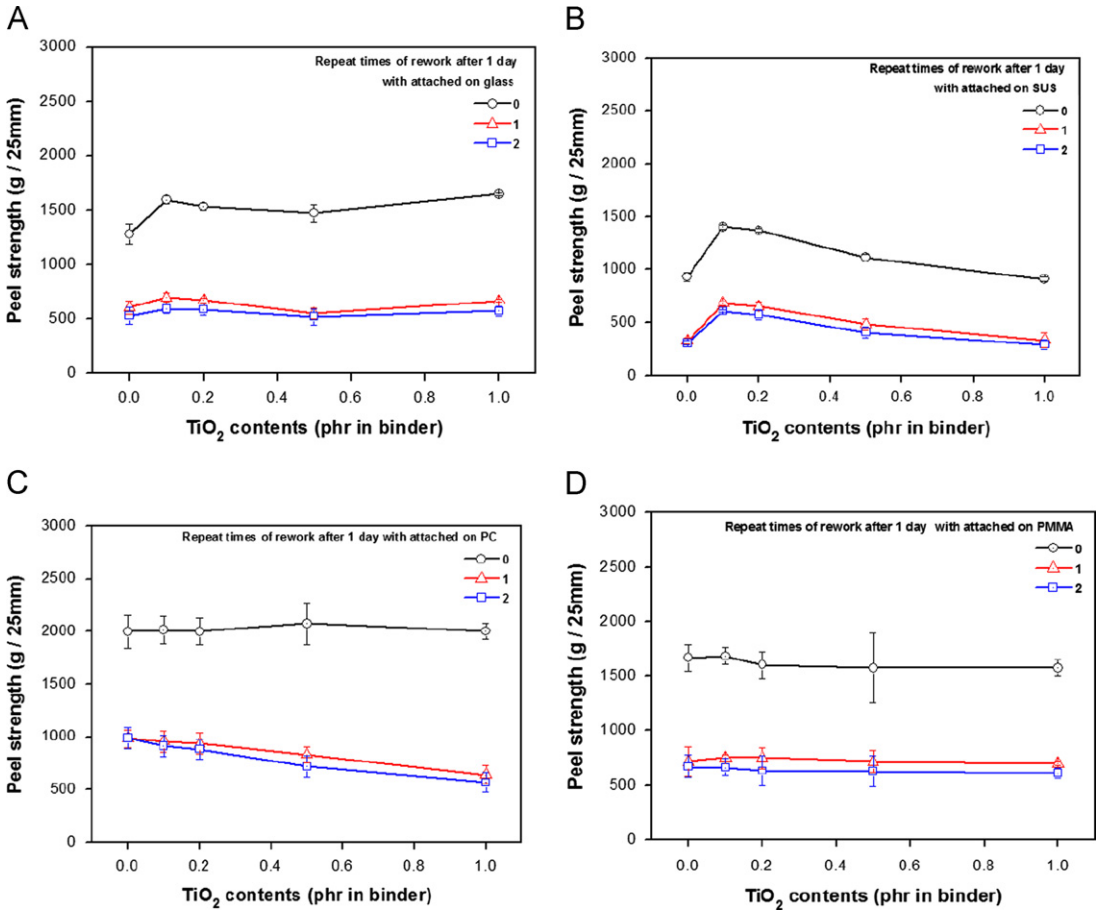

Fig. 10. Peel strength of acrylic PSAs with different TiO_2 contents on glass (A), SUS (3 0 4) (B), PC (C) and PMMA (D) substrates. The measurement was exhibited several times after 1 day with attached on the substrate for re-workability.

property regardless of TiO_2 contents in Fig. 10(D). Moreover, a considerable standard deviation of the samples occurred and this was related to being mixed mode. Mixed mode includes both cohesive and interfacial failure after peeling. This is shown in Fig. 10(C) and (D).

Tack is the second measured adhesive property. Fig. 11(A) shows a decrease in the tack. Tack is an essential adhesion property and it explains the ability of the adhesive to adhere to the substrate in short time and low pressure. Moreover, tack is highly dependent on the polymer molecular mobility [27]. Probe tack of acrylic PSAs reinforced with TiO_2 was affected by the UV irradiation. Because the adhesion area and wetting properties between substrates and adhesives are considered by UV crosslinking. Due to this reason, the maximum value of tack is reduced in adhesives with higher UV dose and this indicates higher crosslinking density. Fig. 11(B) shows a typical stress–strain curve during the debonding process of the probe tack. The strain is obtained by dividing the crosshead displacement by the actual contact area. At comparatively low strains, the curve presents a sharp stress maximum and adhesive debonding. It has a shape that is similar to the stress–strain plots of brittle polymeric materials in the usual tensile tests. In this study, a similar behavior was explained for 1600 dose. On the other hand, if the fibrils debonding from the probe surface by interfacial fracture indicates the stress maximum, a large area under the curve and a high strain at break is observed, the acrylic PSAs have similar with plastic deformation.

The following results were adopted, in the case of shear adhesion failure temperature (SAFT) measurements which are as shown in Fig. 12. Many studies have reported that inorganic materials enhanced the thermal stability of polymer composites as filler [34]. Hence, SAFT measurement is a useful method for explaining the thermal resistance of PSAs. Furthermore, an overall improvement of SAFT was achieved by loading TiO_2 particles into acrylic PSAs. PSAs were reinforced with TiO_2 particles and SAFT increased with an increase in the TiO_2 contents, with a maximal value at 0.5 phr of TiO_2 in binders. This was due to the formation of well-dispersion TiO_2 in polymer matrix. Moreover, this was also attributed to the increase in the storage modulus at room temperature. This suggests improved cohesion of PSA-TiO_2-composites. At the content of TiO_2 1.0 phr in binders, SAFT is apparently decreased. As mentioned above, an increase in the content of TiO_2 particles increased the viscosity. Moreover, high viscosity and agglomerations indicate low wetting property of PSAs-TiO_2 nanocomposites. Meanwhile, it was expected, that the shear strength will increase at higher crosslinking density due to the UV irradiation and this was also studied [35,36].

3.8. *Viscoelastic properties*

The viscoelastic properties of PSAs are associated with the adhesion performance and curing behaviors. This gives us insight into the PSAs characteristics of the PSAs-TiO_2 nano-composites. Moreover, the storage modulus represents the elastic deformation of PSAs and hardness at a given temperature and frequency [37]. But in this study, in order to understand the effect of UV irradiation on the change the viscoelastic properties, the UV irradiation time sweep experiment of pure PSAs and PSAs-TiO_2

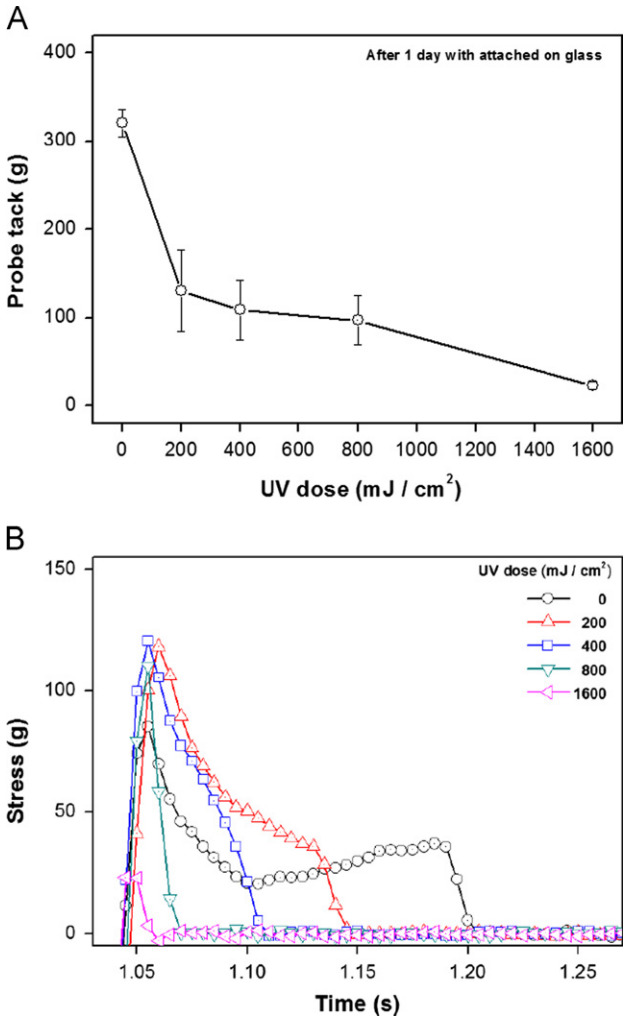

Fig. 11. Prove tack (A) and stress-strain curve (B) of acrylic PSAs with increasing UV dose on a glass substrate.

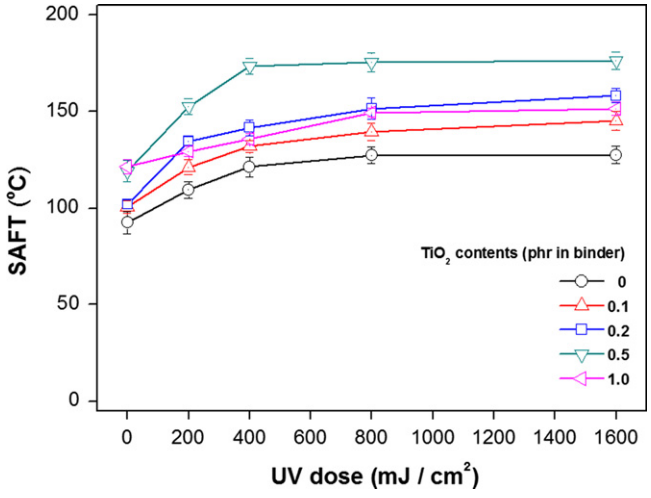

Fig. 12. Shear adhesion failure temperature (SAFT) with increasing UV dose on TiO_2 contents.

nano-composites were conducted. The frequency, strain amplitude and UV intensity are maintained at each test interval and the only variable parameter is the UV irradiation time. Fig. 13 shows the variation of the storage modulus (G′) of pure PSA and PSA-TiO_2 nano-composites as a function of UV irradiation time with a

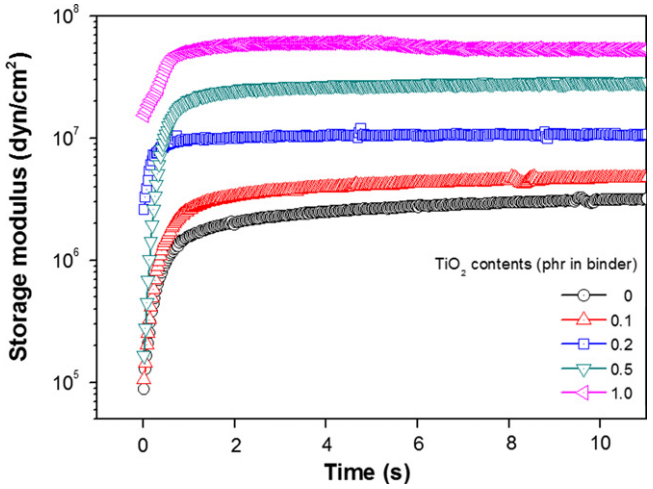

Fig. 13. Variation of storage modulus (G') of pure PSA and PSA-TiO_2 nano-composites as a function of UV irradiation time with a frequency of 1 Hz and 90 mW/cm^2 of UV intensity under a nitrogen atmosphere.

frequency of 1 Hz and 90 mW/cm^2 of UV intensity under a nitrogen atmosphere. When loading TiO_2 particles, stiff filler, to a PSA matrix, soft matrix, the storage modulus increases with increasing TiO_2 contents. Meanwhile, introducing TiO_2 particles into the PSA matrix improved the storage modulus greatly in the rubbery plateau. And storage modulus sharply increased from 0 to 1 s in all the samples. From 1 s forward, only minor change can be observed. Due to this, all samples were subjected to the same extent of UV light exposure that is 1 s at 90 mW/cm^2. These observations can be related to the strong interfacial interactions between the PSA matrix and inorganic materials and they are normally studied in the rubber composites [38,39].

4. Conclusion

Optical properties, UV-curing behaviors and adhesion performance of acrylic PSA based on 2-PEA reinforced with different TiO_2 particles were investigated. The TiO_2 nanoparticles can increase the optical properties such as refractive index. But, at a value of 1.0 phr of TiO_2 in binders' transmittance and gel fraction decreased and this is due to the self-agglomerate and poor dispersion in polymer matrix as shown by FE-SEM observation. Moreover, thermal stability also decreased at a value of 1.0 phr of TiO_2 in binders and this indicates that the high storage modulus has an effect on low wetting properties of PSAs-TiO_2 nano-composites on substrates. In this study, semi-IPN structure using trifunctional acrylate monomer with high refractive index material, a photoinitiator and UV irradiation were employed in order to improve the optical properties and thermal stability of PSAs-TiO_2 nano-composites. The UV-curing behaviors were examined by using FTIR-ATR. The C=C absorbance peak of TAEIs decreased and the conversion was calculated to explain the optimal UV dose. Furthermore, adhesion performance was also measured by peel strength, probe tack regarding re-work properties of use in many optical films. UV-curing behaviors and adhesion performance is the main requirement for PSAs-TiO_2 nano-composites. TiO_2 concentration of 0.5 phr in the binders can give a good balance but 1.0 phr in the binders loading seems too high for the PSAs matrix. Similarly in this study, UV dose of around 400 mJ/cm^2 shows balanced properties.

References

[1] Satas D. Handbook of pressure sensitive technology. 2nd ed.. New York: Van Nostrand-Reinhold; 1989.

[2] Czech Z. Synthesis and cross-linking of acrylic PSA system. J Adhes Sci Technol 2007;21(7):625–35.
[3] Zosel A. Adhesion and tack of polymers: influence of mechanical properties and surface tension. Colloid Polym Sci 1985;263(7):541–53.
[4] Zosel A. Effect of cross-linking on tack and peel strength of polymers. J Adhes 1991;34(1):201–9.
[5] Linder A, Lestriez B, Mariot S, Creton C, Maevis T, Luhmann B, et al. Adhesive and rheological properties of lightly crosslinked model acrylic networks. J Adhes 2006;82(3):267–310.
[6] Czech Z, Loclair H, Wesolowska M. Photoreactivity adjustment of acrylic PSA. Rev Adv Mater Sci 2007;14(2):141–50.
[7] De crevoisier G, Fabre P, Corpart J-M, Leibler L. Switchable tackiness and wettability of a liquid crystalline polymer. Science 1999;285(5431):1246–9.
[8] Tobing SD, Klein K. Molecular parameters and their relation to the adhesive performance of emulsion acrylic pressure-sensitive adhesives, part 2. effect of crosslinking. J Appl Polym Sci 2001;79(14):2558–64.
[9] Tobing SD, Andrew K. Molecular parameters and their relation to the adhesive performance of acrylic sensitive adhesive. J Appl Polym Sci 2001;79 (12):2230–44.
[10] Czech Z. The thermal degradation of acrylic pressure-sensitive adhesives based on butyl acrylate and acrylic acid. Prog Org Coat 2009;65(1):84–7.
[11] Czech Z, Vernetzung von Haftklebstoffen auf Polyacrylatbasis, Wyd. Politechniki Szczecinskiej, Szczecin, 1999.
[12] Park Y-J, Lim D-H, Kim H-J, Park D-S, Sung I-K. UV- and thermal-curing behaviors of dual-curable adhesives based on epoxy acrylate oligomers. Int J Adhes Adhes 2009;29(7):710–7.
[13] Dufour P. In: Fouassier JP, Rabek JF, editors. Radiation curing in polymer science and technology, Vol. 1. London: Elsevier Science Publisher; 1993.
[14] Xiao P, Wang Y, Dai M, Wu G, Shi S, Nie J. Synthesis and Photopolymerization kinetics of benzophenone piperazine one-component initiator. J Polym Adv Technol 2007;19(5):409–13.
[15] Bayramoglu G, Kahraman MV, Kayaman-Apohan N, Gungor A. Synthesis and characterization of UV-curable dual hybrid oligomers based on epoxy acrylate containing pendant alkoxysilane groups. Prog Org Coat 2006;57(1):50–5.
[16] Kayaman NA, Demirci R, Cakir M, Gungor A. UV-curable interpenetrating polymer networks based on acrylate/vinylether functionalized urethane oligomers. Radiat Phys Chem 2005;73(5):254–62.
[17] Joo H-S, Park Y-J, Do H-S, Kim H-J, Song S-Y, Choi K-Y. The curing performance of UV-curable semi-interpenetrating polymer network structured acrylic Pressure-sensitive adhesives. J Adhesion Sci Technol 2007;21(7):575–88.
[18] Auchter G, Aydin O, Zettl A, Satas D. In: Satas D, editor. Handbook of pressure sensitive adhesive technology. Warwick, RI: Satas Associates; 1999. p. 444–514.
[19] Gao J, Yang M, Lei J. Surface organic modification of titanium dioxide fine particles through photo polymerization. J Appl Polym Sci 2012;124 (6):5286–92.
[20] Chang EP. Electrooptical light-management material: low-refractive-index adhesives. J Adhes 2007;83(1):15–26.
[21] Miyamoto M. Control of refractive index of pressure-sensitive adhesives for the optimization of multilayered media. Jpn J Appl Phys 2007;46(6B):3978–80.
[22] Joo H-S, Do H-S, Park Y-J, Kim H-J. Adhesion performance of UV-cured semi-IPN structure acrylic pressure sensitive adhesives. J Adhes Sci Technol 2006;20 (14):1573–94.
[23] Yuan HG, Kalfas G, Ray WH. Suspension polymerization. Polym Rev 1997;31 (2):215–99.
[24] Do H-S, Park Y-J, Kim H-J. Preparation and adhesion performance of UV-crosslinkable acrylic pressure sensitive adhesives. J Adhesion Sci Technol 2006;20(13):1529–45.
[25] Kajtna J, Likozar B, Golob J, Krajnc M. The influence of the polymerization on properties of an ethylacrylate/2-ehtyl hexylacrylate pressure-sensitive adhesive suspension. Int J Adhes Adhes 2008;28(7):382–90.
[26] Kajtna J, Golob J, Krajnc M. The effect of polymer molecular weight and crosslinking reactions on the adhesion properties of microsphere water-based acrylic pressure-sensitive adhesives. Int J Adhes Adhes 2008;29(2):186–94.
[27] Kajtna J, Krajnc M. UV crosslinkable microsphere pressure sensitive adhesives-influence on adhesive properties. Int J Adhes Adhes 2011;31(1):29–35.
[28] Chau JLH, Lin Y-M, Li A-K, Su W-F, Chang K-S, Hsu SL-C, et al. Transparent high refractive index nanocomposite thin films. Materials Letters 2007;61 (14):2908–10.
[29] Zisman WA. Relation of the equilibrium contact angle to liquid and solid constitution. Advances in Chemistry Series 1964;43:1–51.
[30] Fox H, Zisman WA. The spreading of liquids on low energy surfaces. I. polytetrafluoroethylene. Journal of colloid science 1950;5(6):514–31.
[31] Kawabe M, Tasaka S, Inagaki N. Effect of surface modification by oxygen plasma on peel adhesion of pressure-sensitive adhesive tape. J Appl Polym Sci 2000;78(7):1392–401.
[32] Sohn S. Various ways to control the bulk properties of pressure sensitive adhesives. J Adhes Sci Technol 2003;17(5):703–23.
[33] Kajtna J, Sebenik U. Microsphere pressure sensitive adhesive acrylic polymer/montmorillonite clay nanocomposite materials. Int J Adhes Adhes 2009;29 (5):543–50.
[34] Hu. X, Xhang W, Si M, Gelfer M, Hsiao B, Rafailovich M, et al. Dynmics of polymers in organosilicate nanocomposites. Marcromolecules 2003;36 (3):823–9.
[35] Czech Z. New copolymerizable photoinitiators for radiation curing of acrylic PSA. Int. J Adhes Adhes 2007;27(3):195–9.
[36] Czech Z, Wojciechowicz M. The crosslinking reaction of acrylic PSA using chelate metal acetylacetonates. Eur Polym J 2006;42(9):2153–60.
[37] Lim D-H, Do H-S, Kim H-J. PSA performances and viscoelastic properties of SIS-based PSA blends with H-DCPD tackifiers. J Appl Polym Sci 2006;102 (3):2839–46.
[38] Maiti S, De SK, Bhowmick AK. Quantitative estimation of filler distribution in immiscible rubber blends by mechanical damping studies. Rubber Chem Technol 1992;65:293–302.
[39] Roy D, Bhowmick AK, De SK. Anisotropy in mechanical and dynamic properties of composites based on carbon fiber filled thermoplastic elastomeric blends of natural rubber and high density polyethylene. Polym Eng Sci 1992;32(14):971–9.